Supporting Information

Riffell et al. 10.1073/pnas.0910592106

SI Text

Behavioral Experiments. The headspace volatiles from *D. wrightii* and *A. palmeri* flowers and mixtures of synthetic odorants were tested for their effects on the anemotactic flight and foraging behavior of male moths in a laboratory wind tunnel (Plexiglas, length × width × height = 4.0 × 1.5 × 1.5 m). Air was forced into the upwind end of the tunnel through a carbon filter and exhausted at the downwind end through a duct vented into a laboratory fume hood. As measured with a 3D sonic anemometer (81000; RM Young Co.) sampling at 32 Hz, the wind speed was 25 cm/s, and turbulent wind intensities of 0.004 N/m^2 occurred along the principal (u) axis. Male moths were tested individually by introduction into the wind tunnel, in a wire cage covered at both ends by plastic Petri plates, on a platform located near the downwind end of the tunnel. After a 1.5-min acclimation period, the Petri plates were removed to release the moth, and it was allowed to fly for 5 min, after which it and the tested odor mixture were replaced. Mixtures were tested in semirandom order; the wind tunnel was cleaned with ethanol between treatments and a control test (mineral oil, no odor) was performed in between treatments. In each day of testing two to four moths per stimulus were exposed to the positive (*D. wrightii* floral odor) or negative (no odor) controls. Each synthetic mixture was tested by pipetting 10 μL of the solution (in odorless mineral oil) onto a conical paper flower similar to those of Raguso and Willis (1), made from #4 filter paper (Whatman). Equal volumes of mineral oil were used as negative controls. Serving as positive control, a freshly cut *D. wrightii* flower or *A. palmeri* umbel was placed in a sealed 3-L glass jar outside of the wind tunnel. Charcoal-filtered air was pumped into the jar at 0.02 L/min and conducted from the jar through 2 m of Teflon tubing (2 mm i.d.) to a paper flower in the wind tunnel. Floral scent at this flow rate produced emissions from artificial flowers similar to those from natural flowers (2). We had previously identified nine odorants from the *D. wrightii* floral scent that, together in a mixture but not singly, were as behaviorally effective as the natural floral scent (3). To identify the minimal number of components from the nine-component mixture that could evoke flight behavior, single components were removed from the mixture, and the behavioral effectiveness of the resulting reduced mixture was tested in the wind tunnel (Table S4). Concentrations and ratios of mixture components were scaled to those found in the *A. palmeri* and *D. wrightii* floral headspaces. These concentrations were initially determined on the basis of Raoult's Law and the concentration within the mixture and volatility of each component, and then verified and adjusted empirically by using gas-tight syringes (5 mL) and quantification by GC-FID. Concentrations of constituents in the mixtures and emission rates were further quantified and adjusted by pipetting 10 μL of an individual mixture solution onto a paper flower in a 3-L glass jar. To collect volatiles emitted by a floral source held in the glass jar, a collection system (Analytical Research Systems) was used to pull the headspace air from the jar through a sorbent-cartridge trap at a flow rate of 2 L air/min for 12 h (traps and headspace analysis described below). Trapped volatiles then were eluted from the cartridge with hexane (600 μL) and analyzed by using GC-FID. Headspace collections from *D. wrightii* and *A. palmeri* flowers were similarly collected and analyzed to allow comparisons of the constituent concentrations, ratios, and total emissions between mixtures and floral bouquets. Based on the concentrations and volatilities of its constituents, the total pressure of each mixture was calculated and expressed in mm Hg.

Two types of behavioral data were acquired from the wind-tunnel experiments: (*i*) video acquisition and subsequent motion analysis of flight behavior for each treatment group (detailed below), and (*ii*) scoring of moth behaviors (see Table S2). Video images of flight tracks were captured by an overhead CCD camera with a macrolens (4 × 4-m area) and recorded as analog video. The video was digitized and analyzed with a video-acquisition and motion-analysis system (Peak Motus 3D v7.2; Vicon) and the resulting 2D flight tracks were analyzed for ground speed and orientation (track angle) relative to the odor source defined as the 0° origin. Transit-probability surface plots, derived from superimposed flight trajectories, were used to show the variation of flight tracks (4). Transit plots were calculated from 2D views of the wind tunnel divided into 1,367 64-cm^2 squares. For each olfactory stimulus, the occurrences of a moth within each square were summed and divided by the total number of occurrences to yield a probability of occupancy of the square. The angular distribution of moth orientation relative to the odor source (0°) is shown by the histogram on the right of each surface plot in Fig. 1. For the two-choice tests in the wind tunnel, an attraction index was calculated from the number of proboscis extensions (probes) into the flower corollas by $(\#\text{Probes}_{\text{FlowerA}} - \#\text{Probes}_{\text{FlowerB}})/(\text{Total } \#\text{Probes})$.

Collection of Floral Scent. Scent was collected from *D. wrightii* and *A. palmeri* flowers by using dynamic headspace sorption (2, 5). The floral headspace collections allowed us to scale the emission rates of the synthetic mixture constituents to those of the flowers. To accomplish this, living flowers in field populations were enclosed in transparent vinyl oven bags (Reynolds) cinched at 500-mL volumes with plastic ties. Portable diaphragm pumps (10D1125; Gast Manufacturing) were used to pull fragrant headspace air through sorbent cartridge traps at a flow rate of 500 mL/min. Traps were constructed by packing 100 mg of Super Q adsorbent (mesh size 80–100; Alltech) in borosilicate glass tubes (7 mm) plugged with silanized glass wool. Scent collections began at anthesis (near sunset for all plants) and continued overnight for up to 12 h. Ten replicates of floral volatiles were collected from 10 individuals of *D. wrightii* or *A. palmeri*.

Odor Analysis. Trapped volatiles were eluted from sorbent cartridges by using 600 μL of HPLC-grade hexane. Each sample was stored in a 2-mL borosilicate glass vial with a Teflon-lined cap at −80 °C until analysis. Volatile sample (1 μL) was analyzed by using a GC–TOF-MS system consisting of an HP 6890 (Agilent Technologies) GC and a Waters TOF-MS. GC columns (J&W Scientific) used were DB1 (30 m, 0.25 mm, and 0.25 μm) and DB5 (30 m, 0.25 mm, and 0.25 μm), and helium was used as carrier gas at constant flow of 1 cc/min. The initial oven temperature was 50 °C for 5 min, followed by a heating gradient of 6 °C/min to 230 °C, which was held isothermally for 6 min. Peaks were identified by using TOF-MS with 70-eV electron-impact ionization. Chromatogram peaks were identified tentatively with the aid of the NIST mass spectral library (≈120,000 spectra) and verified by chromatography with authentic standards (when available) or known components of essential oils. Peak areas for each compound were integrated by using MicroMass MassLynx software (Waters) and are presented in terms of relative abundance as percentage of total fragrance emitted. Peak area for each odorant was quantified by using either an

internal standard (*n*-nonyl acetate) or through a five-point standard (0.1 ng to 1 mg) of the synthetic odorants and expressed in units of ng per flower per h. The *A. palmeri* and *D. wrightii* floral scents contain between 63 and 82 odorants, respectively (2, 5). In this study, we examined only peaks that elicited significant neural responses (*z*-scores $\geq$ 2.0).

Electrophysiology. ***Experimental preparation.*** Adult male moths (*M. sexta*; Lepidoptera: Sphingidae) were reared in the laboratory on an artificial diet (6) under a long-day (17/7-h light/dark cycle) photoperiod and prepared for experiments 2–3 days after emergence, as described (7, 8). In preparation for recording, the moth was secured in a plastic tube with dental wax, leaving the head and antennae exposed. The head was opened to expose the brain, and the tube was fixed to a recording platform attached to the vibration–isolation table. The preparation was oriented so that both ALs faced upward, and the tracheae and sheath overlying one AL were carefully removed with a pair of fine forceps. The brain was superfused slowly with physiological saline solution [150 mM NaCl, 3 mM $CaCl_2$, 3 mM KCl, 10 mM *N*-Tris(hydroxymethyl) methyl-2 aminoethanesulfonic acid buffer, and 25 mM sucrose, pH 6.9] throughout the experiment.

Olfactory stimulation. Olfactory stimuli were delivered to the preparation by two different methods. The first method used a gas chromatograph. A 1-μL sample of collected headspace volatiles was injected (splitless, 30 s) into a Shimadzu model 14A GC equipped with a flame ionization detector and a DB-1 column (J&W Scientific). Effluent was split 1:1 between the flame ionization detector of the GC and the moth antenna by using a universal glass Y connector (J&W Scientific). Deactivated, fused-silica capillary tubing of the same internal diameter as the separation column carried the effluent to each detector. Effluent to the antenna passed through a heated transfer line (Syntech) set at 250 °C into a 16-mm (i.d.) glass odor-delivery tube, via a small side hole, and mixed with a stream of charcoal-filtered, humidified air flowing through the delivery tube to the side of the antenna at a rate of 800 mL/min.

In the second method (9), pulses of air from a constant air stream were diverted through a glass syringe containing a piece of filter paper bearing floral odorant. The stimulus was pulsed by means of a solenoid-activated valve controlled by an electronic stimulator (W-P Instruments). The outlet of the stimulus syringe was positioned 2 cm from and orthogonal to the center of the antennal flagellum ipsilateral to the AL of interest. Stimulus duration was 200 ms, and five pulses were separated by a 5-s interval. Four classes of olfactory stimuli were used: (*i*) aromatics, benzyl alcohol (*Bol*), methyl salicylate (*Mal*), and benzaldehyde (*Bea*); (*ii*) monoterpenoids, (±) linalool (*Lin*), nerol (*Ner*), β-myrcene (*Myr*), and geraniol (*Ger*); (*iii*) sesquiterpeniods, farnesene (*Far*) and caryophyllene (*Car*); and (*iv*) aliphatics, ethyl sorbate (*Esb*), propyl valerate (*Pvl*), ethyl tiglate (*Etg*), and butyl butyrate (*Bbu*). The control solvent for synthetic floral volatiles and mixtures was odorless mineral oil (control) and for the floral extracts, it was hexane (*Hex*). A total of 14 adult moths were used in multiunit recording experiments (detailed below). The first six moths (n = 78 units) were exclusively used in GC-MR experiments and stimulated with the effluent from the GC. The next eight moths (n = 111 units) were stimulated with synthetic odor stimuli. Two series of *D. wrightii* mixture stimuli were prepared. In the first mixture series, individual odorant concentrations were maintained equal to those within the original nine-component mixture and thus total mixture concentrations differed from one another. A second series of experiments controlled for the differences in total mixture concentration where the relative ratios of components within the mixtures were the same as in the nine-component blend, but the component concentrations were elevated such that the total mixture concentrations were equal to one another.

Ensemble recording. The odor-evoked responses of 189 units were obtained in 14 male moths. Recordings were made with 16-channel silicon multielectrode recording (MR) arrays (a 4 × 4–3 mm 50–177; NeuroNexus Technologies). The spatial distribution design of this MR (a 4 × 4 array) suits the dimensions of the AL in *M. sexta* (Fig. S6*A*). These probes have four shanks spaced 125 μm apart, each with four recording sites 50 μm apart. The MR was positioned under visual control by using a stereo microscope (Fig. S6*B*). The four shanks were oriented in a line parallel to the antennal nerve, with the first shank inserted into the macroglomerular complex and the remaining shanks elsewhere in the AL (Fig. S6 *A* and *C*). The MR was advanced slowly through the AL by using a micromanipulator (Leica Microsystems) until the uppermost recording sites were just below the surface of the AL. Thus, the four shanks of the MR recorded from four regions of glomerular neuropil across the AL. Ensemble activity was recorded simultaneously from the 16 channels of the MR array by using two Lynx-8 amplifiers (Neuralynx). Spike data were extracted from the recorded signals and digitized at 25 kHz per channel by using Discovery acquisition software (Data Wave Technologies) and a 2821-G 16SE analog-to-digital board (Data Translation,) on a personal computer platform (Data Wave Technologies). Filter settings (typically 0.6–3 kHz) and system gains (typically 5,000–20,000) were software adjustable on each channel. Spikes were sorted by using a clustering algorithm based on the method of principal components (PCs) (Off-line Sorter; Plexon). Only those clusters that were separated in 3D space (PC1–PC3) after statistical verification (multivariate ANOVA; $P < 0.05$) were used for further analysis (11–16 units were isolated per ensemble; n = 14 ensembles in as many animals). Spikes arising from the same unit were recorded at adjacent recording sites, thus providing geometric information about the spatial origin of the signals. Each spike in each cluster was time-stamped, and these data were used to create raster plots and calculate peristimulus time histograms (PSTHs), interspike interval histograms, cross-correlograms, and rate histograms. All analyses were performed with Neuroexplorer (Nex Technologies) using a bin width of 5 ms, unless noted otherwise.

Data Analysis. ***Unit responses to GC-eluate.*** As in Riffell et al. (2), the control corrected response for every unit to the GC eluates was quantified by calculating a RI. RI values reflect the deviation from the mean response of all units across all odors in one ensemble, as:

$$\mathrm{RI} = (R_{odorant} - R_m)/\mathrm{SD}, \qquad [1]$$

where $R_{odorant}$ is the number of spikes evoked by the test odorant minus the number of spontaneous spikes (averaged over three 400-ms time intervals during the GC run when no eluate was emitted from the column), R_m is the mean response, and SD is the standard deviation across the data matrix. The RI values for the nonresponsive units fell between −2.0 and + 2.0, based on the cumulative sum (CUMSUM) test. Given that 50% (on average) of recorded units in each ensemble were unresponsive, R_m approximated the background activity level, and thus negative values of the RI indicated response suppression. The RI values for all units were color-coded and arranged as an activity matrix with each row representing the ensemble response to a different odor stimulus. The RI had a range from −3.0 SDs (inhibited units; cool colors) to +3.0 SDs (strongly excited units; warm colors). Because there was such variability in the time frame of maximum unit responses with respect to the onset of the GC-peak, we used a sliding 400-ms time window during the GC peak to determine when units gave a significant response (> mean spontaneous activity).

Temporal analysis of odor-evoked activity. Sorted units were arranged according to which of the four AL shanks (I–IV) defined by the

MR yielded each recording. For each unit sorted, PSTHs were generated for all responses to each odor stimulus and the control (solvent only) stimulus. The response windows were defined as the 100-ms period beginning at the onset of the 200-ms stimulus pulse and continuing in 100-ms bins to the following 200-ms odor pulse (5-s interstimulus interval). A unit was considered to be responsive if its control-subtracted PSTH was above (excitatory) or below (inhibitory) the 95% confidence limits derived from the CUMSUM test.

Mean firing rate and mean instantaneous firing rate responses. Within each time window (10–1,000 ms) we quantified the response for every unit by calculating the mean firing rate of its response. The mean firing rate was based on the number of spikes evoked by the test stimulus within the predetermined time window. The mean instantaneous firing rate for each unit was the mean inverse of the interspike interval within the predetermined time window.

Pattern of ensemble synchrony and net synchrony. To calculate the temporal relationship between each pair of units, we used a cross-correlation analysis using the following formula:

$$\mathrm{SI\%} = \frac{[\mathrm{SE}]_{\mathrm{RAW}} - [\mathrm{SE}]_{\mathrm{SHUFFLED}}}{\mathrm{N}_1(\mathrm{T}) + \mathrm{N}_2(\mathrm{T})} \times 100, \qquad [2]$$

where $[\mathrm{SE}]_{\mathrm{RAW}}$ is the number of coincident events in the 5-ms cross-correlogram peak centered around $t = 0$, and $[\mathrm{SE}]_{\mathrm{SHUFFLED}}$ is the number of coincident events after trial shuffling (shift predictor method) to correct for coincidence attributable to chance and an increased firing rate (10). The corrected correlograms were calculated by averaging over four trial shifts and subtracting the result from the raw correlogram. T is the total response time over which spikes were counted (10–1,000 ms), and N_1 and N_2 are the total number of spikes recorded from units 1 and 2 during time T. The synchrony index (SI%) therefore reflects the percentage of synchronous spikes relative to the total number of spikes recorded from the two neurons. All calculations were implemented in Matlab 7.02 (Mathworks) or Neuroexplorer (Nex Technologies). To visualize the stimulus-dependent synchrony pattern within an ensemble, we arranged individual units in a circular array used to describe ensemble patterns (7, 11). Each pair of units was connected with a line that depicted the magnitude of the correlation (SI%): values 10–15%, dotted line in Fig. 4; values 15–20%, dashed line in Fig. 4; values 20–30%, dashed line in Fig. 4; and values >30%, solid line in Fig. 4.

In addition to the pattern of ensemble synchrony, the number of synchronous spikes produced by the entire ensemble, or the net synchrony, was determined. The net synchrony was calculated by summing the number of synchronous spikes produced by the ensemble, in 5-ms bins, after shuffle subtraction. The mean number of synchronous spikes was determined over a predetermined time window (10–1,000 ms).

Multivariate analysis of odor classification, neural codes, and behavior. The ensemble responses were examined through time in multivariate space and correlated with behavior similarly transformed in multivariate space. Each neural code (mean firing rate, mean instantaneous firing rate, and pattern of ensemble synchrony) of the ensemble was transformed into a vector and analyzed by cluster analysis to determine the Euclidean distances (d) between stimuli, calculated by:

$$d_{ij} = \sqrt{\sum_{k=1}^{p} (X_{ik} - X_{jk})^2}, \qquad [3]$$

where i and j indicate odors, p is the number of dimensions, i.e., units, and X_{ik} is the response in unit k to odor i. Population data were calculated only within, not between, ensembles. The origin of the Euclidean distances between stimuli was set to the *D. wrightii* extract. Ensemble Euclidean distances were normalized to the maximum to produce a dissimilarity index (0–1.0), which allowed comparison between stimuli. Similarly, the Euclidean distances in behavioral responses between olfactory stimuli were determined. Behaviors included in this analysis were the mean percentage feeding responses, flower contact, flower diving, approach, close hover, upwind flight, average time of successful feeding response, flight speed, number of proboscis extensions, and time spent feeding (Table S2). Results from the multivariate analysis on the behavioral results produced Euclidean distances between pairs of odor stimuli, thus allowing direct correlation between the dissimilarity indices of the neural codes and behavior.

A stepwise multiple regression analysis (both forward and backward) was used to examine the neural codes as sources of variation (R) in the behavioral results. An important consideration is the intercorrelation between the neural codes (the independent variables in the stepwise multiple regression analysis). A partial correlation analysis was conducted on the neural codes yielding regression coefficients (r) ranging from −0.08 to 0.20. Moreover, to identify whether rate codes (mean instantaneous firing rate and mean firing rate) or synchrony codes (pattern of ensemble synchrony and net synchrony) may be correlated to one another, and thus not accurately be represented in the stepwise multiple regression analysis, each neural code was individually removed from the analysis and the results were compared with the multiple regression model that included all variables. Removal of mean instantaneous firing rate and net synchrony did not influence the first two steps of the stepwise regression analysis, thus indicating that multicollinearity may not be a significant factor in this analysis.

The classification analysis used the behavioral response to the odor panel as the template and the neural responses to the same odor panel were used as tests. The dissimilarity indices between test (behaviorally effective and ineffective mixtures) and template stimulus were computed, and responses were assigned to the nearest neighbor. Responses were drawn from the time period of odor stimulation (200 ms), and the percentage of success of odor identity was the fraction of correct assignments over the total number of assignments. The response time bins were 10–1,000 ms. To examine the time scales in which classification success was greatest for the mean rate and the pattern of ensemble synchrony, a fast Fourier analysis was conducted on the time series (10-ms time bins) of the percentage of classification success from the beginning to end of a 1,000-ms duration from odor onset. For all analyses, values were calculated only within, and not between, preparations.

Histological identification of recording probe locations. To examine the precise location of the recording probes, the brain was excised and immersed in 1–2% glutaraldehyde in 0.1 M phosphate buffer to increase tissue contrast and facilitate location of probe tracks. Brains ($n = 8$) were fixed for 6–12 h, then dehydrated with a graded ethanol series, cleared in methyl salicylate, and finally imaged as whole mounts with a laser-scanning confocal microscope (Zeiss 510 Meta equipped with a 457-nm argon laser). Optical sections at 1 μm and this method reliably revealed the tracks of the four MR shanks in the AL without the need for tissue staining. To examine consistency of the MR probe position in the AL, confocal image stacks were reconstructed and analyzed by using Amira v.4.1.2 (Indeed-Visual Concepts). Glomerular structures in the AL were labeled as described (12, 13) with the boundaries between adjacent glomeruli determined by the 4viewer mode that allows assessment of the glomerular structure in all possible 2D planes of each respective image stack. The glomeruli adjacent to, and impaled by, each shank were color-coded: blue for shank 2, yellow shank 3, and green for shank 4. Shank 1 was inserted in the MGC region of the AL. In

addition, the MGC glomeruli (Cumulus, C-MGC, and Toroids 1 and 2, T-MGC) were reconstructed. The relative positions of the labeled sexually isomorphic glomeruli with respect to the MGC glomeruli allowed comparison between preparations. 3D reconstructions of the impaled and neighboring glomeruli enabled determination of the consistency between preparations on the location of the recording sites. Although identification of individual glomeruli is an important prerequisite for assigning functional significance to a given glomerulus, it was beyond the scope of this study.

1. Raguso RA, Willis MA (2005) Synergy between visual and olfactory cues in nectar feeding by wild hawkmoths, *Manduca sexta. Anim Behav* 69:407–418.
2. Riffell JA, et al. (2008) Behavioral consequences of innate preferences and olfactory learning in hawkmoth–flower interactions. *Proc Natl Acad Sci USA* 105:3404–3409.
3. Riffell JA, Lei H, Christensen TA, Hildebrand JG (2009) Characterization and coding of behaviorally significant odor mixtures. *Curr Biol* 19:335–340.
4. Frye MA, Tarsitano M, Dickinson MH (2003) Odor localization requires visual feedback during free flight in *Drosophila melanogaster*. *J Exp Biol* 206:843–855.
5. Raguso RA, Henzel C, Buchman SL, Nabhan GP (2003) Trumpet flowers of the Sonoran Desert: Floral biology of *Peniocereus* cacti and sacred *Datura. Int J Plant Sci* 164:877–892.
6. Bell RA, Joachim FG (1976) Techniques for rearing laboratory colonies of tobacco hornworms and pink ballworms. *Ann Entomol Soc Am* 69:365–373.
7. Christensen TA, Pawlowski VM, Lei H, Hildebrand JG (2000) Multiunit recordings reveal context-dependent modulation of synchrony in odor-specific neural ensembles. *Nat Neurosci* 3:927–931.
8. Lei H, Christensen TA, Hildebrand JG (2004) Spatial and temporal organization of ensemble representations for different odor classes in the moth antennal lobe. *J Neurosci* 24:11108–11119.
9. Christensen TA, Waldrop BR, Harrow ID, Hildebrand JG (1993) Local interneurons and information processing in the olfactory glomeruli of the moth *Manduca sexta*. *J Comp Physiol [A]* 173:385–399.
10. Aertsen AM, Gerstein GL, Habib MK, Palm G (1989) Dynamics of neuronal firing correlation: Modulation of ''effective connectivity.'' *J Neurophys* 61:900–917.
11. Wilson MA, McNaughton BL (1994) Reactivation of hippocampal ensemble memories during sleep. *Science* 265:676–679.
12. Galizia CG, McIlwrath SL, Menzel R (1999) A digital three-dimensional atlas of the honeybee antennal lobe based on optical sections acquired by confocal microscopy. *Cell Tissue Res* 295:383–394.
13. Huetteroth W, Schachtner J (2005) Standard three-dimensional glomeruli of the *Manduca sexta* antennal lobe: A tool to study both developmental and adult neuronal plasticity. *Cell Tissue Res* 319:513–524.

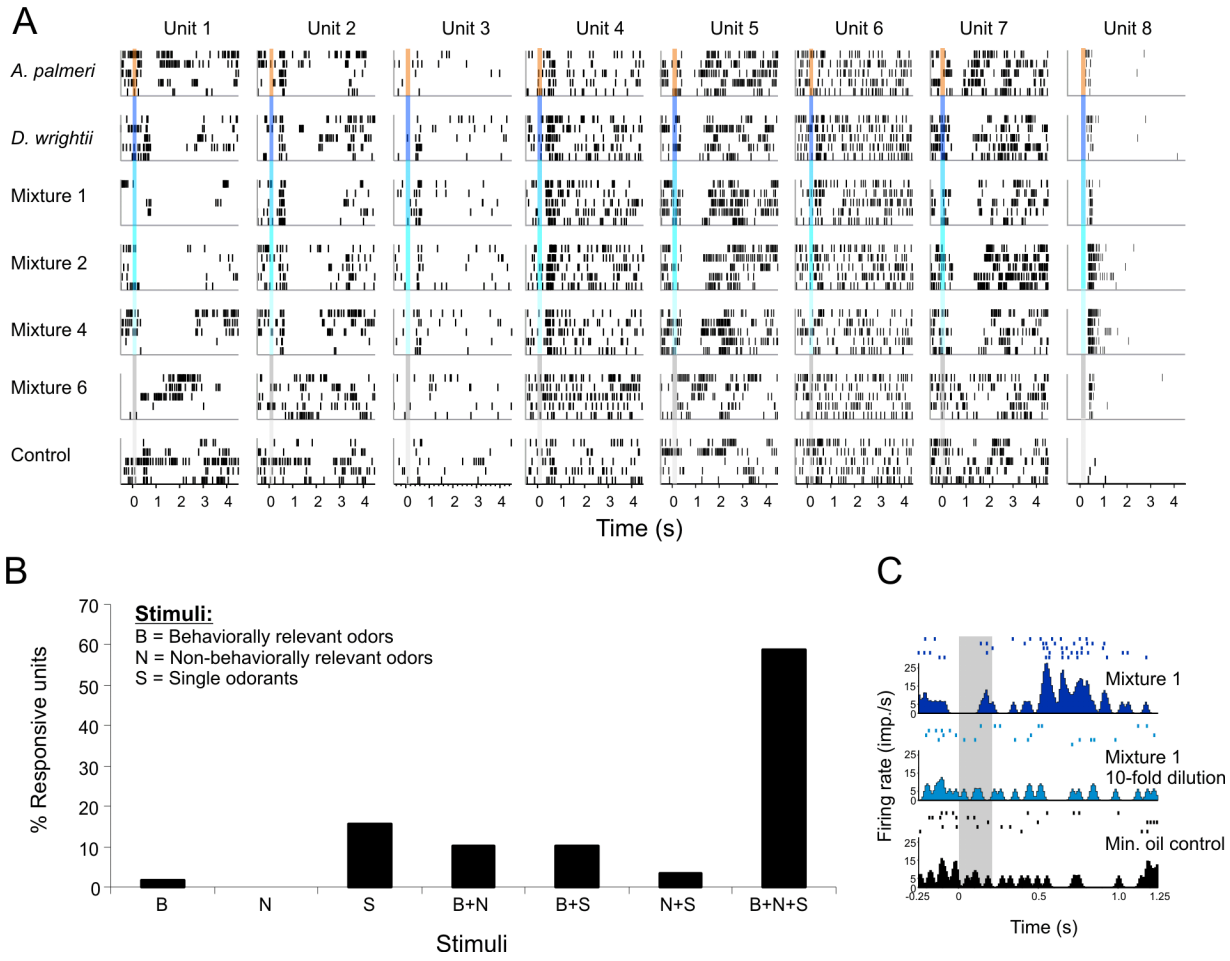

Fig. S1. Characteristics of individual unit responses to the different odor stimuli. (*A*) Representative raster plots of individual unit responses (columns) to the different mixture stimuli (rows). Shaded areas denote the 200-ms odor mixture stimulation. Bottom row is the mineral oil control. Stimulus order was randomized within a given preparation. (*B*) Percentage of units that exhibited selective responses to behaviorally effective (B), behaviorally ineffective (N), and single-odorant (S) stimuli and nonselective responses to two or more of these stimuli classes. (*C*) Peri-event histograms and rasters of the single unit (out of all responsive units) that selectively responded to behaviorally effective mixtures (*Top*, blue). This unit, however, did not significantly respond to a 10-fold lower concentration of the behaviorally effective mixture 1 (*Middle*, blue), which elicited the same level of activity as the mineral oil (no odor) control (*Bottom*, black).

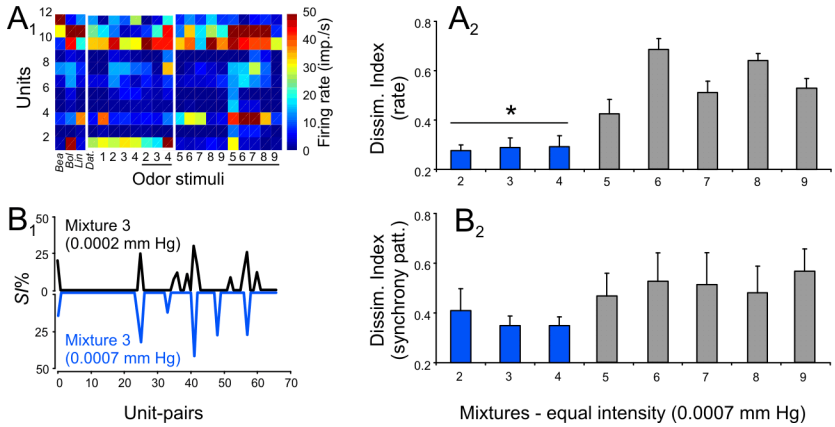

Fig. S2. Population responses from behaviorally effective and ineffective mixtures and mixtures with equal intensity. (A_1) Ensemble firing rate responses to single odorants *Bea*, *Bol*, and *Lin*, and mixtures 1–9 at dissimilar and equal (underlined numbers) intensities. (A_2) The dissimilarity indices from the population-level responses based on mean firing rate to behaviorally effective and ineffective mixtures (mixtures 2–9), but all at the same intensity as mixture 1. (B_1) The synchrony coefficients for all unit-pairs in a single preparation ($n = 66$ unit pairs) to mixture 3 (black line; 0.0002 mm Hg) and mixture 3 at the same intensity as mixture 1 (blue line; 0.0007 mm Hg). (B_2) The dissimilarity indices from the population-level responses based on the pattern of ensemble synchrony to behaviorally effective and ineffective mixtures (mixtures 2–9), all at the same intensity as mixture 1. Asterisk denotes a significant difference between odor stimuli ($P < 0.05$).

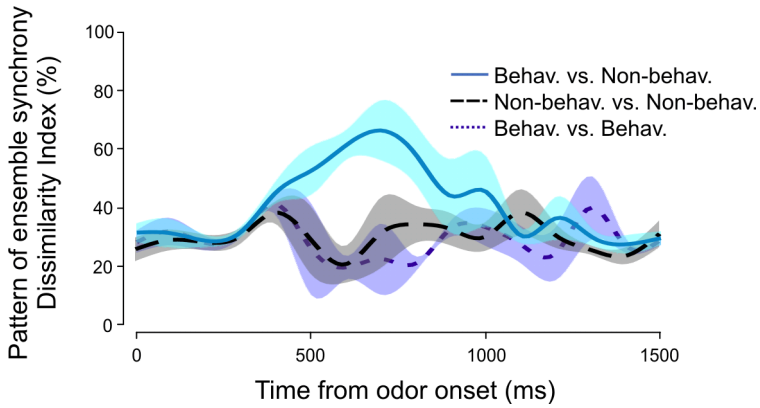

Fig. S3. Dissimilarity indices from the pattern of ensemble synchrony evoked between odor stimuli through time from odor onset (200-ms odor pulse at time = 0 ms) for one preparation. Dissimilarity indices between behaviorally effective and ineffective mixtures (light blue solid line), ineffective mixtures to one another (dashed black line), and behavioral mixtures to one another (dotted dark blue line) are shown. Shaded areas denote the ± SEM.

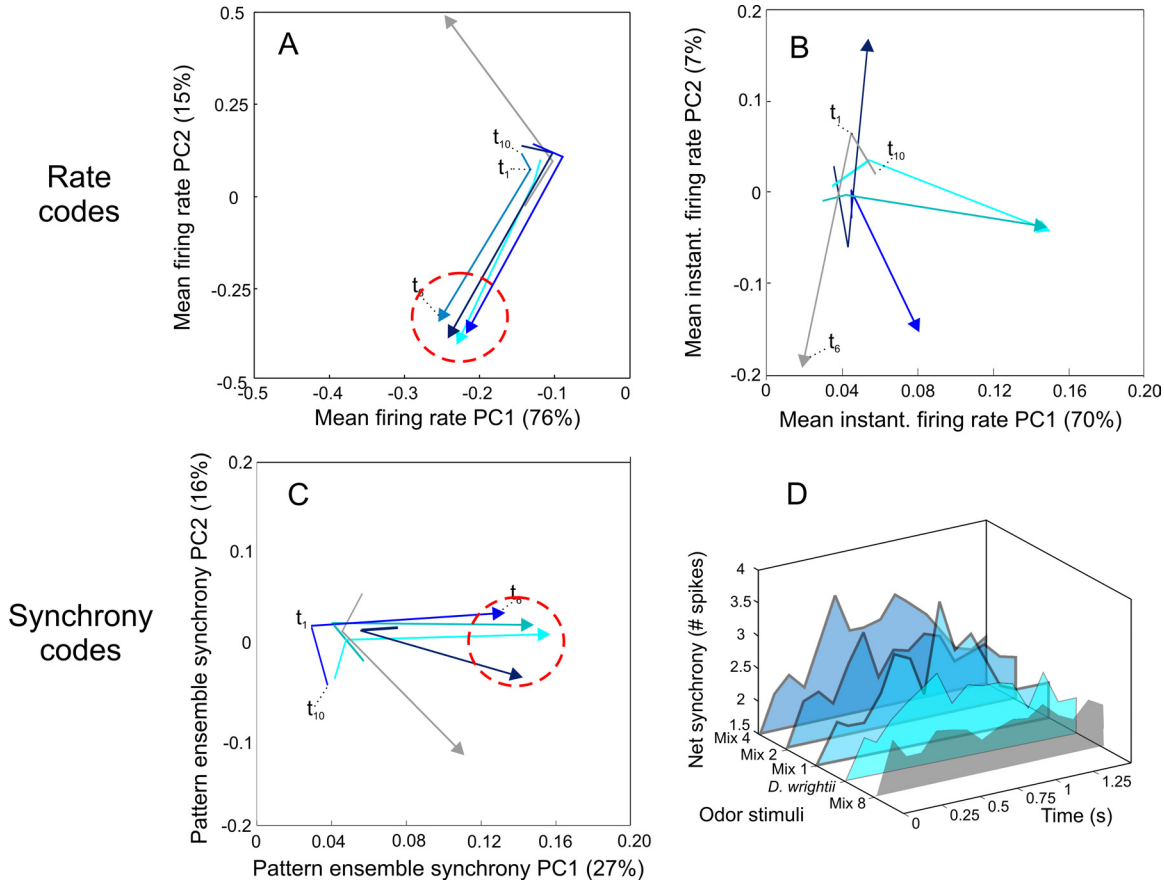

Fig. S4. Population trajectories of each neural code: mean firing rate, mean instantaneous firing rate, pattern of ensemble synchrony, and net synchrony. Five different odors are shown, four of which elicited significant behavioral responses (in blue), and one that did not elicit behavioral responses (gray). Three time points are shown for the ensemble response of each odor stimulus: t_1 the first 100 ms before odor encountering the antenna (origin of the responses), t_6, the 600 ms after odor contacted the antenna; and t_{10}, the 1 s after odor delivery. Arrows denote the time period of odor stimulation. (*A*) The population trajectories of the mean firing rate responses. (*B*) The population trajectories of the mean instantaneous firing rate responses. (*C*) Population trajectories of the pattern of ensemble synchrony evoked responses to the different mixture stimuli. (*D*) Net synchrony to a behaviorally effective (blue areas) and ineffective (gray area) mixture through time (the odor pulse begins at 0 ms). The dashed red circles in *A* and *C* denote similar population responses to the behaviorally effective stimuli.

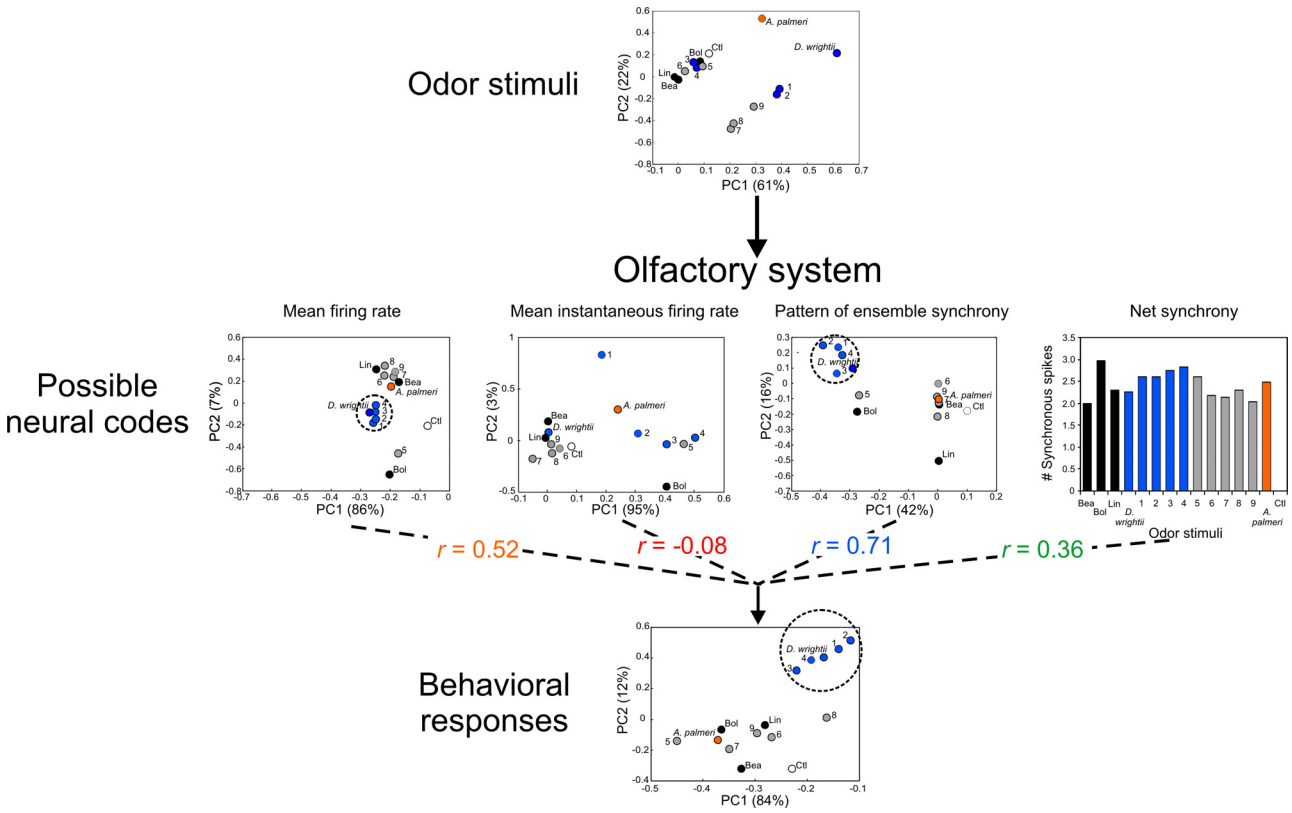

Fig. S5. Comparison of odor-stimulus complexity with the ability of the olfactory system to organize the odors into behavioral percepts. PCAs were conducted on the olfactory stimuli (concentration of the shared odor stimulus constituents, total odor emission rate), the neural codes from a single ensemble (mean firing rate, mean instantaneous firing rate, pattern of ensemble synchrony, and net synchrony), and behavioral responses to generate the coefficient plots (see *Materials and Methods* for further details about olfactory stimuli, analysis of ensemble data, and elicited behavioral responses). Circles are color-coded according to behavioral efficacy of the odor stimuli: blue (behaviorally effective), gray (ineffective), orange (*A. palmeri* odor), single odorants (black; *Bea*, *Bol*, and *Lin*), and mineral oil control (white). The correlation coefficients between the behavioral responses and the neural codes are shown beside the arrows. Dashed circles denote distinct clustering of behaviorally effective mixtures.

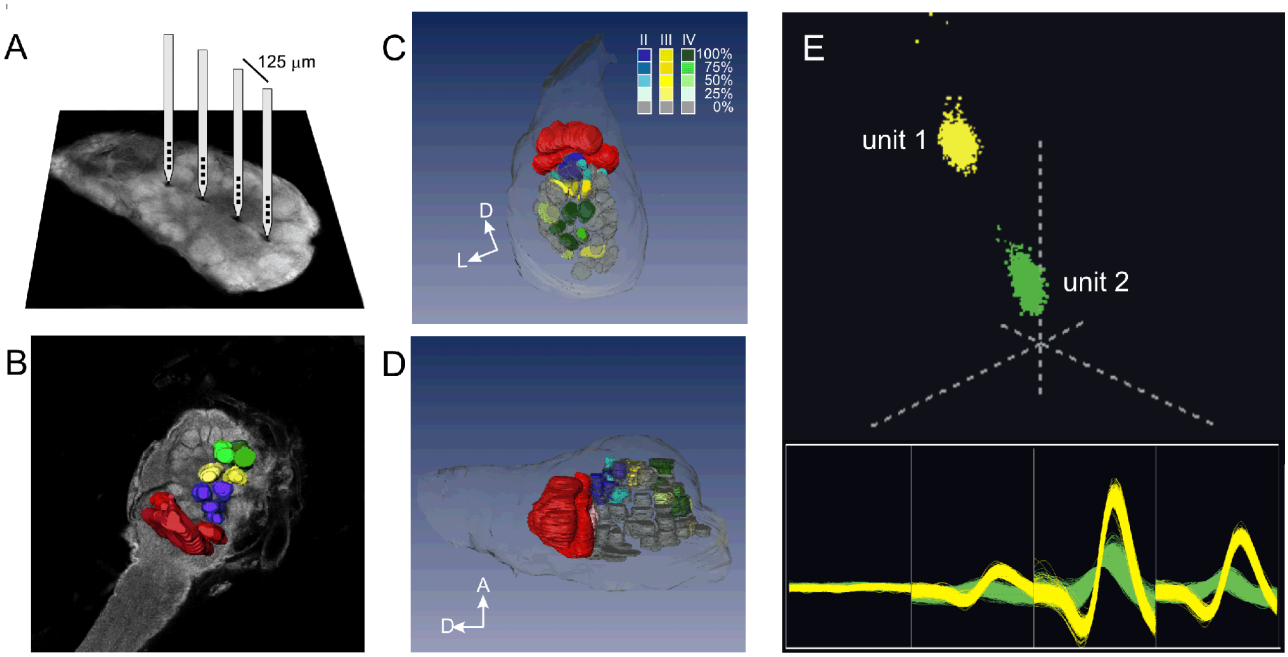

Fig. S6. Position of MR array in the moth's AL and sorting of recorded units. (*A*) The four shanks are spaced such that the array encompasses a large volume of the AL. (*B*) A confocal stack image demonstrating the middle portions of the AL. Glutaraldehyde fixation of the AL and confocal microscopy enabled determination of the positions of each of the MR shanks and the depth to which the MR was inserted into the AL. (*C* and *D*) From confocal image stacks, the glomeruli penetrated by or adjacent to MR shanks could be determined for each preparation. The cumulative placement of the MR probe for all eight preparations is shown. Blue glomeruli correspond to shank II, yellow for shank III, and green for shank IV. Shank I was placed in the MGC-T1 (MGC shown in red). The position of the probe was consistent between preparations as demonstrated by the impaled glomeruli occupying the lateral region of the AL and the depth in which the probe was placed in the AL. The MR shanks were consistently placed in the lateral side of the AL at a posterior-to-anterior depth of ≈200 μm. The color scale denotes the frequency that glomeruli were impaled or adjacent to the shanks for all preparations, e.g., deep blue glomeruli correspond to those glomeruli being impaled by shank II 100% of the time (8/8 of the preparations). Glomeruli not located near the shanks are shown in white. (*E*) Neural activity was recorded on each of the four channels, plotted in 3D (*Upper*), and sorted according to waveform characteristics (*Lower*).

Table S1. Liquid-phase constituent concentrations used in behavioral and electrophysiological experiments

Mixture	Odorant	Concentration, μg	Purity, % (source)
Synthetic *D. wrightii*	Benzaldehyde (*Bea*)	0.50	≥99.5 (Fluka)
	Benzyl alcohol (*Bol*)	12.77	≥99.8 (Sigma)
	Methyl salicylate (*Mal*)	0.67	≥99.5 (Fluka)
	β-Myrcene (*Myr*)	0.44	≥95.0 (Fluka)
	(±)Linalool (*Lin*)	0.90	≥97.0 (Aldrich)
	Nerol (*Ner*)	1.86	≥97.0 (Aldrich)
	Geraniol (*Ger*)	75.70	≥99.0 (Fluka)
	E-Caryophyllene (*Car*)	0.84	≥98.5 (Fluka)
	Farnesene (Far)	0.44	≥90.0 (Fluka)
Synthetic *A. palmeri*	Benzaldehyde (*Bea*)	0.75	≥99.5 (Fluka)
	β-Myrcene (*Myr*)	0.80	≥95.0 (Fluka)
	Ethyl tiglate (*Etg*)	0.40	>98.0 (SAFC)
	(*E,E*)-Ethyl 2,4-hexadienoate (*Esb*)	56.5	≥97.0 (Aldrich)
	Propyl valerate (*Pvl*)	3.05	>98% (MPBio)
	Butyl butyrate (*Bbu*)	0.80	>98.0 (Spectrum Co.)

Table S2. Behavioral results to the different mixture stimuli

Behavioral metric	Mixture stimuli 1	2	3	4	5	6	7	8	9	*D. wrightii* flower	Mineral oil control
Upwind flight (%)	86.3	90.9	90.9	81.8	77.2	59.0	59.0	59.0	63.6	86.3	22.7
Approach (%)	81.8	86.3	86.53	81.8	68.1	45.4	54.5	50.0	59.0	81.8	22.7
Close hover (%)	68.1	77.2	63.6	77.2	50.0	27.2	36.3	22.7	36.3	72.7	13.6
Contact (%)	63.6	63.6	54.5	54.5	36.3	22.7	18.1	18.1	22.7	63.6	9.0
Feeding (%)	45.4	54.5	45.4	45.4	18.1	9.0	9.0	9.0	13.6	54.5	0
Probes (#/moth)	2.2	2.4	2.1	2.0	0.7	0.3	0.2	0.5	0.6	2.4	0
Flower dive (#/moth)	0.13	0.13	0.09	0.13	0	0	0	0	0	0.13	0
Foraging bout (s)	7.64	13.36	8.73	8.18	3.82	0.91	1.64	1.82	3.27	10.82	0
Flight speed (cm/s)	17.83	22.16	19.4	26.92	37.19	56.44	68.24	57.97	63.55	23.71	67.25
Time to feeding (s)	56	42	123	84	228	129	174	69	143	76	0
Dissimilarity index (to *D. wrightii*)	0.09	0.09	0.12	0.14	0.51	0.63	0.59	0.59	0.69	NA	0.92

NA, not available.

Table S3. Stepwise regression identifying the neural predictors of behavior in *M. sexta* moths to behaviorally effective and ineffective odor mixtures

Behavioral predictor	Step	β	R	τ	P
Synchrony pattern	1	0.42	0.39	5.61	4.6e-8
Mean firing rate	2	0.26	0.46	4.30	2.3e-5
Mean net synchrony	3	0.13	0.48	2.33	0.02
Variable not included:					
Mean instantaneous firing rate	NA	0.06	NA	1.00	0.31

NA, not available.

Table S4. Quantification of emission rates

Odor source	Emission rate (ng/h)
D. wrightii flower	93.64 (14.84)
Benzaldehyde (*Bea*)	0.1 (0.01)
Benzyl alcohol (*Bol*)	8.75 (3.38)
Linalool (*Lin*)	0.24 (0.12)
Mixture 4 (*D. wrightii* mimic)	6.27 (0.07)
Benzaldehyde (*Bea*)*	0.22 (0.07)
Benzyl alcohol (*Bol*)*	5.78 (0.11)
Linalool (*Lin*)*	0.26 (0.07)

Emission rates (ng/h) of constituents in the synthetic mixtures were scaled to those of the *D. wrightii* flower (verified by GCMS and GC-FID). $N = 10$ flowers from 10 *D. wrightii* plants and 10 paper flowers loaded with the synthetic mixtures. Values in parentheses are SEM.

*Constituent emission rates are not significantly different from *D. wrightii* floral emissions (one-way ANOVA: $F_{1,20} = 0.29$, $P = 0.59$).